Desalination and Water Treatment
www.deswater.com

doi: 10.5004/dwt.2017.20126

62 (2017) 360–368
February

Removal of phenol and chromium (VI) using hydrotalcite synthesized from lab acid wastewater

S. Martínez-Gallegos*, J. Illescas, J.C. González, G. Macedo, C. Muro-Urista, M.C. Díaz-Nava

División de Estudios de Posgrado, Instituto Tecnológico de Toluca, Av. Tecnológico S/N Ex Rancho La Virgen, Metepec, México, C.P. 52140; emails: soniakorn@yahoo.com (S. Martínez-Gallegos), fillescasm@toluca.tecnm.mx (J. Illescas), jgonzalezj@toluca.tecnm.mx (J.C. González), macedomiranda@yahoo.com (G. Macedo), cmurou@toluca.tecnm.mx (C. Muro-Urista), mdiazn@toluca.tecnm.mx (M.C. Díaz-Nava)

Received 28 February 2016; Accepted 31 July 2016

ABSTRACT

Hydrotalcite-like compounds, also known as layered double hydroxides (LDH) are synthetic compounds that have been widely researched due to their many potential applications. These compounds are usually produced by a co-precipitation method that requires a metallic solution. Some previous works have reported the use of wastewater in LDH synthesis. This paper proposes a sustainable way to reduce waste in the lab. First, hydrotalcite-like compounds were synthesized using wastewater from metal analyses and then they were applied for phenol and chromium removal. In this process, a highly metallic acid residue has not been previously tested in LDH synthesis. It is first reported herein. The obtained materials were characterized and the results demonstrated that LDH with Mg-Al or Zn-Al structures were achieved and that the acidic features from lab wastes do not affect LDH production. The hydrotalcite-like compounds were also thermally treated and reconstructed, indicating that the memory effect appeared to play an important role in phenol and chromium VI adsorption. The thermally treated LDH with Mg-Al adsorbs 111 mg phenol/g and 5.92 mg Cr(VI)/g. Finally, both pollutants were used to prove that the synthesized LDH-like compounds could be used as an adsorbent.

Keywords: Hydrotalcite-like compound; Lab acid wastewater; Co-precipitation method; Memory effect; Adsorption

1. Introduction

Pollution in groundwater is a significant problem for many countries [1]. Nowadays, there is a tendency to combine industrial effluents for treatment of hazardous, non-hazardous, metal and/or organic compounds because it is financially profitable. Phenol and chromium (VI), which come from wastewater discharged by industrial activities, have been intensively studied. Chromium (VI) is a toxic, carcinogenic, mutagenic, harmful substance [2]. Meanwhile, phenol is an aromatic organic compound and an important precursor to many useful materials; it causes severe health effects in the nervous system, kidneys, and liver in humans [3]. Therefore, in this work phenol and chromium (VI) were selected as the target of toxic organic and inorganic pollutants. Conventional methods of removing both compounds from water include reverse osmosis, ion exchange, phytoremediation, bioaccumulation, oxidation-reduction, and coagulation/precipitation [3,4]. Adsorption remains an effective and widely used physicochemical method to remove pollutants from water [5]. A variety of materials have been studied as adsorbents of phenol and chromium VI from aqueous solutions, including corn cob silica-alginate beds [1], ferric oxide nanoparticles [6], water hyacinth and *Bacilus* sp. [2], and carbon foam [7]. Hydrotalcites and their thermally treated products have attracted attention of the scientific community because of their low cost, high adsorption capacity, and unique structure [5].

* Corresponding author.

1944-3994/1944-3986 © 2017 Desalination Publications. All rights reserved.

Hydrotalcites are an important class of inorganic functional material and are considered to have great potential, since they have applications in different areas, such as catalysis, adsorption processes, medicine, adsorptive flotation, flame retardance, and acid scavenging in polymer composites [8,9]. Natural hydrotalcite (HT) has the formula $Mg_6Al_2(OH)_{16}CO_3{\cdot}4H_2O$, which comes from the general equation $\left[M^{2+}_{1-x}M^{3+}_{x}(OH)_2\right]^{x+}(A^{n-})_{x/n}\cdot mH_2O$, where M^{2+} is a divalent ion, such as Mg^{2+}, Co^{2+} or Zn^{2+}, etc.; M^{3+} is a trivalent ion: Al^{3+}, Cr^{3+}, Fe^{3+}, etc.; and $A^{n-}_{x/n}$ is the interlamellar charged anion, for example CO^{2-}_3, SO^{2-}_4, OH^-, Cl^-. This compound is also known as layered double hydroxide (LDH), anionic clays, or hydrotalcite-like compound, when Mg and Al are replaced by other metal ions [9,10].

The thermal decomposition of HT or LDH can be described as a two-step mechanism. When the HT is heated in air at 500°C, it is transformed into a mixture of metal oxides with a high specific area; in this case, the resultant solid can be reconstructed by simple hydration [11]. In the HT, heated in air up to 1,000°C, the structure results in a large amount of pores and induces aluminum-magnesium ($MgAl_2O_4$) spinel formation [12].

There are different methods of synthesizing HT, namely hydrothermal (H), sol-gel (SG), and co-precipitation (CP). The last two (SG and CP) give a product with high specific area, whereas the first two (H and SG) produce a small crystal [13]. The co-precipitation method is the most common technique for obtaining these compounds, and it allows a good yield product to be obtained. It starts with the preparation of an aqueous solution of magnesium and aluminum salts [12].

On the other hand, metal analysis by atomic absorption spectrometry (AS) is based on the generation of metal atoms and their measurement. The metal solution for measurement in this technique is required to be adjusted with nitric acid (2%) until pH is less than 2. The lab wastewater produced in this analysis was very acidic. It is commonly treated by a pH control (pH = 8–10) to precipitate the metal compound until its concentration is under the maximum limits allowed in Mexican regulations, so the precipitate can be deposited in a disposal site.

The purpose of this study is to prepare HT by the co-precipitation method using lab acid wastewater and to probe it for phenol and chromium (VI) removal. Furthermore, it is important to take advantage of the flexibility in the co-precipitation method to obtain HT using acid wastewater from AS, which sometimes includes a large metal species. This method offers hydrotalcite with defined properties. However, since this work uses acid wastewaters collected separately from aluminum and zinc, the produced HT was synthesized only with these metal ions. Finally, it is noteworthy that HT synthesis obtained from the lab acidic wastes has not been reported. Also, the acid conditions in wastewater were due to nitric acid used to preserve samples; therefore, it was necessary to track the behavior of the thermal-treated products and to identify whether any change in their structure occurred due to the incorporation of other species in the HT structure.

2. Experimental

2.1. HT synthesis

Hydrotalcites were synthesized in the laboratory using analytical-grade chemicals obtained from Sigma-Aldrich and used as received. The hydrotalcite products were synthesized by the co-precipitation method.

The used acid wastewater solutions have 1,000 mg/L of aluminum or zinc ions. This concentration corresponds to the metal standard solution used in AS. Each lab acid wastewater solution was enriched using analytical-grade chemicals to reach the necessary mol concentration for hydrotalcite synthesis. The pH value of the lab acid wastewater solution was 1, which is the minimum necessary to maintain metal ions in a solution, and it remained so even when analytical-grade chemicals were added. In order to evaluate the use of the lab acid wastewater containing only aluminum and zinc, first it was verified that the Mg-Al hydrotalcite had not shown structural changes, and then it was confirmed that the Zn-Al hydrotalcite-like compound had been synthesized from the lab acid wastewater, even though common magnesium metal ions were not present in the structure. Both hydrotalcite-like compounds must be used in the removal process.

The hydrotalcite-like compound Mg-Al molar ratio 2 (HTM) was prepared by dropwise addition of an aqueous solution containing 0.1 mol of Mg $Mg(NO_3)_2{\cdot}6H_2O$ 99.8% and 0.05 mol of $Al(NO_3)_3{\cdot}9H_2O$ 98.4%, both dissolved in the lab acid wastewater with only 1,000 mg/L of aluminum. These solutions were added dropwise in an aqueous solution containing 0.1 mol of Na_2CO_3 99% [14].

The hydrotalcite-like compound Zn-Al molar ratio 2 (HTZ) was prepared with the same method using a similar concentration. Therefore, 0.1 mol of $Zn(NO_3)_2{\cdot}6H_2O$ 98% was dissolved in acid wastewater containing 1,000 mg/L of Zn and 0.05 mol of $Al(NO_3)_3{\cdot}9H_2O$ 98.4%. In both cases, pH value was kept at 10 by addition of an aqueous (2 M) NaOH 98% solution.

The obtained precipitate was aged for 24 h under the same synthesis conditions. Finally, it was repeatedly washed with deionized water.

2.2. Thermal treatment of HTM and HTZ

The obtained samples, HTM and HTZ were thermally treated at different temperatures, from 300°C to 1,000°C for 3.5 h under air atmosphere in order to evaluate the structural changes in the hydrotalcite-like compounds and their thermal products (HTMC and HTZC).

2.3. Al and Zn analyses

To confirm the incorporation of Al or Zn into the HTM or HTZ, different water samples, used to wash the hydrotalcites, were analyzed to identify aqueous-metal species such as Zn and Al, using acetylene-air flame/atomic absorption (Thermo) with single-element hollow cathode lamps. Calibration curves were prepared from stock solutions for each element, Al or Zn. These metals were chosen for lamp bulb availability.

2.4. X-ray diffraction

Powder X-ray diffraction (PXRD) diagrams were recorded in a Siemens D-500 instrument using Ni filtered Cu Kα radiation (λ = 1.54050 Á) with a scanning speed of 2° (2θ)/min and equipped with Diffract AT software. Patterns

were collected in the range of 5°–70° with a two-step size 0.017° and a rate of 30 s per step. Samples were prepared as a finely pressed powder in aluminum sample holders.

2.5. TG analyses

Thermal decomposition of the hydrotalcite was carried out in a Linseis SPA 1600 incorporated high thermogravimetric analyzer. 10 mg of sample were heated in an open alumina crucible at a rate of 10°C/min up to 1,000°C. After thermal treatment, the hydrotalcites were kept in a desiccant, thus the mass losses were calculated as a percentage on a dry basis.

2.6. FTIR spectra

Infrared spectra (FTIR) were obtained at room temperature with a Varian 640-IR spectrometer equipped with an ATR diamond. The resolution was 4 cm^{-1}.

2.7. Surface area and SEM

The morphologies of HTM and HTZ were examined at 20 kV with a scanning electron microscope (SEM) in a JEOL model JSM5900-LV fitter with an energy dispersive X-ray analyzer (EDAX-Oxford). The BET surface area and mean pore diameter and total pore volume were determined by N_2 adsorption at 77 K using a BELSORP Max instrument. The samples were heated at 100°C for 6 h before surface areas were measured.

2.8. Adsorption test

Phenol and chromium (VI) adsorption was conducted on the hydrotalcite-like compound thermally treated at 550°C (HTMC or HTZC) and was measured by batch equilibrium techniques at several LDH quantities from 20 to 200 mg (adsorption isotherm). The suspensions [sorbent and phenol (50 mg/L, C_6H_6O Baker) or chromium (VI) (10 mg/L, K_2CrO_4 Mallinckrodt)] were shaken at room temperature, after an adequate, previously determined time (2 h).

The adsorbed amounts were determined from the initial (C_i) and final or equilibrium (C_e) concentrations of the pollutant solution. The adsorption isotherms were described quantitatively by applying the equation:

$$C_s = \left(C_i - C_e\right)\frac{V}{m} \tag{1}$$

where C_e is the solute (adsorbate) concentration in the solution at equilibrium (mg/L), C_s is the amount of solute adsorbed in the solid at equilibrium (mg/L), V represents the volume of dissolution for batch contact, and m is the HT mass.

2.9. Phenol and chromium (VI) determination

The supernatants were filtered to determine the pollutant concentration by UV-vis absorbance in the 510 nm region for phenol (prepared by the antipiridine method) and 540 nm for chromium (VI) (prepared by the 2,4 diphenil carbazide method). The spectrophotometric measurements were recorded using a Genesys 10 UV-visible spectrophotometer.

3. Results and discussion

3.1. Metal analyses

The chemical analyses of Al or Zn ionic metals in lab acid wastewater and water washings used in the HTM or HTZ synthesis are shown in Table 1.

For both samples, HTM and HTZ, the Al metallic ion was monitored for lamp availability. In the case of the HTZ, at first, the determined Zn concentration was 2,229 mg/L. From this quantity, 1,000 mg/L came from acid wastewater. After the synthesis, this concentration decreased to 5.89 mg/L, which is below the allowable limit (6 mg/L) established by Mexican law [15]. Furthermore, in the same sample, Al concentration at the beginning of the synthesis was 4,709 mg/L. This value corresponded to the quantity of chemical reagent ($Zn(NO_3)_2{\cdot}6H_2O$) plus aluminum content in lab acid wastewater. At the end of the process, Al concentration was 40.68 mg/L, representing less than 1% of the original concentration. This means that more than 99% of the aluminum was taken for HTZ precipitation.

As for the HTM sample, it was determined to be at 3,359 mg/L before starting with the preparation method. This concentration decreased to 8.09 mg/L; that is, almost 99.5% of the metal was taken for HTM precipitation. It is important to mention that these values are out of regulation, since Mexican laws have established 0.20 mg/L for Al [16]. However, these are low concentrations in the case of laboratory treatment wastewater. In both cases, the layered double hydroxides (LDH) have taken the anion of interest to form hydrotalcite-like compounds of Mg-Al and Zn-Al. Consequently, this observation has given rise to the second purpose of this work; that is, wastewater treatment from the atomic absorption analyses obtained.

In this case, a selection has been made between Zn and Al, which were selected for collection from the acid wastewater to make sure that both metal ions were taken to build the hydrotalcite structure and every metal took part in the octahedral form that constituted a lamellar HT compound. There was no real difference between the Al or Zn ions coming from the analytical grade chemicals or metal standard solution (lab acid wastewater) because both of them were precipitated during the HT precipitation method. Thus, hydrotalcite synthesis by co-precipitation has proved to be a viable option to treat metal wastewater generated in lab research, since it reduces the amount of metal deposited into the discharges and possibly the environment.

3.2. Powder X-ray Diffraction

The most common hydrotalcite was Mg-Al with carbonate as a counterion in the interlamellar space. In order

Table 1
Chemical analyses for metal solution mixed with metal wastewater

Sample	Metal concentration (mg/L)			
	Al initial	Al final	Zn initial	Zn final
HTM	3359	8.09	—	—
HTZ	4709	40.68	2229	5.89

to confirm that the Al metal ions coming from lab acid wastewater did not have a real influence on the hydrotalcite behavior, the HTM sample was thermally treated at different temperatures and then its structure was reconstructed only with water. The X-ray diffraction patterns of the synthesized HTM, their calcinated solids from the lab metal acid wastewater solution and their reconstructed products showed the general features of all hydrotalcite-like compounds (Fig. 1(a)). HTM displayed a well-crystallized hydrotalcite-like structure, with sharp, symmetric reflections (003, 006, 110, and 113 planes), as well as wide, asymmetric reflections (012, 015, and 018 planes). All of these reflections are characteristic planes of hydrotalcite-like compounds. These results indicate that neither intensity nor crystallinity differences were observed from the XRD patterns of the synthesized solids from the lab acid wastewater solutions [17]. In the case of thermally treated HTM at 400°C, 500°C, and 600°C, two main peaks associated to MgO can be observed, which were the only crystalline phase mixed oxides that were identified (Fig. 1(a)). When the samples were heated at 700°C or 800°C, a periclase-like material was obtained, too. Finally, at 1,000°C the sample was crystalline, and only MgO and $MgAl_2O_4$ spinel were observed [17]. Lastly, reconstructed hydrotalcites are shown in Fig. 1(b). All structures exhibit broader peaks than the original sample, since the reconstructed hydrotalcite corresponds to the rhombohedral polytype [18]. No other formation was observed in the reconstruction process, so only the memory effect for HT was present in this step. This effect is associated with carbonate ions in interlamellar space [19]; meanwhile, nitrate ions in the solution due to the acidification stage were not incorporated into the HT structure, so the memory effect is not altered.

The d_{003} values correspond to the basal spacing of two consecutive brucite-like hydroxide layers in HTM. Table 2 shows three main d spacings corresponding to the HTM and reconstructed samples. These values were close to the same three major peaks reported by Cavani [20] (7.8, 3.9, and 2.6 Å) for this anionic clay in the 5°–70° 2θ range. No relationship was found between the temperature of the treated sample and the d spacing calculated for the reconstructed samples. Also, this spacing corresponds to carbonate ions in the interlayer space, so no other species were included in the interlayer space. Likewise, the hydrotalcite Mg-Al molar ratio of 2 d_{003} = 7.64 is very close to the same molar ratio reported in a other work (d_{003} = 7.7) [21]. Thus, electrostatic interactions between layer and interlayer anions were the same for all samples, and the amount of Al in each sample was very close to that in the brucite-type sheet. The reconstruction capacity of the hydrotalcite-like compound cannot be lost when lab acid wastewater is used in the synthesis process. However, in the case of samples thermally treated at 800°C and 1,000°C, the main structure corresponds to a spinel compound. In this case, only a small peak for the HT compound is detected; therefore, the intensity of d_{003} spacing decreases at higher treated temperatures, possibly indicating a dissolution reaction in HTM-medium. Assuming a value of 4.77 for the width of the brucite sheet [22] and subtracting it from the width of the HTM unit layer (7.64 Å, derived from the first basal reflection d_{003}), the thickness of the interlayer region can be calculated. Hence, the obtained value was 2.87 Å, which is in concordance with a CO_3^{2-} ion lying parallel to the Mg-Al

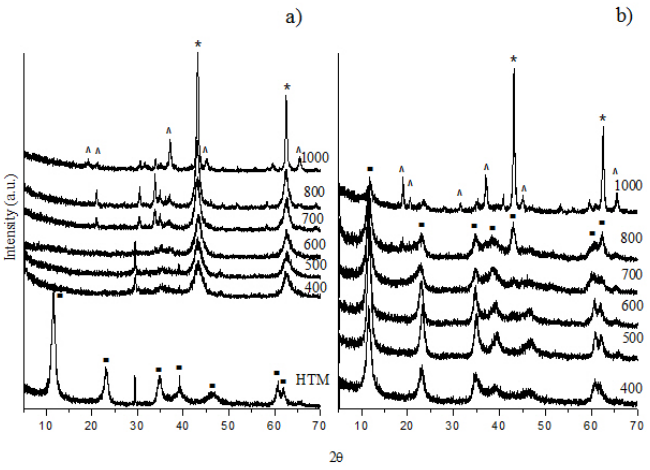

Fig. 1. X-ray diffraction patterns for thermally treated and reconstructed HTM products.
Note: ■ – hydrotalcite; * – MgO; and ^ – $MgAl_2O_4$.

Table 2
d spacings for HTM and reconstructed samples

Calcined sample (°C)	d spacings (Å)		
	d_{003}	d_{006}	d_{012}
HLM	7.64	3.82	2.56
400	7.60	3.85	2.57
500	7.53	3.82	2.57
600	7.61	3.85	2.58
700	7.64	3.87	2.57
800	7.60	3.85	2.58
1,000	7.45	3.75	2.53

sheets and strong hydrogen bonding. Also, the d_{003} = 7.64 Å was in agreement with a Mg-Al molar ratio 2 reported in the literature [21]. As for the samples thermally treated at 400°C, 500°C and 600°C, a shift was found towards lower values; this is because some carbonate ions were replaced by OH ions, closer brucite layers [19].

On the other hand, for HTZ it is important to verify the incorporation of the Zn metal ion into the HT structure. The original HTZ including its thermally treated and reconstructed products are presented in Fig. 2. For this sample, no diffraction peaks that were characteristic of the other solids were detected in any of the patterns. Consequently, this indicated that the Zn^{2+}-Al^{3+}-CO_3^{2-} hydrotalcite-like compound was the only crystalline precipitated product. Similarly, for the reconstructed sample, a mixed metal oxide and a typical structure of HT were detected.

The d_{003} spacing in the HTZ and the reconstructed sample were affected by thermal and reconstructed treatments because of the change from 7.43 to 5.86 Å. This could be due to a dissolution reaction into the sample or to the crystallization of ZnO formed during thermal treatment [23]. Nevertheless, this structure is not observed in the HTZC sample; therefore, the layer of the HT was close in the reconstructed sample.

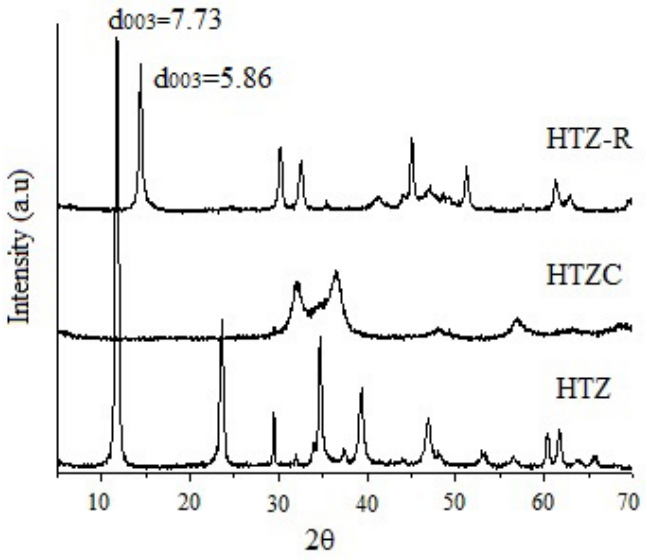

Fig. 2. X-ray diffraction patterns for thermally treated and reconstructed HTZ products.

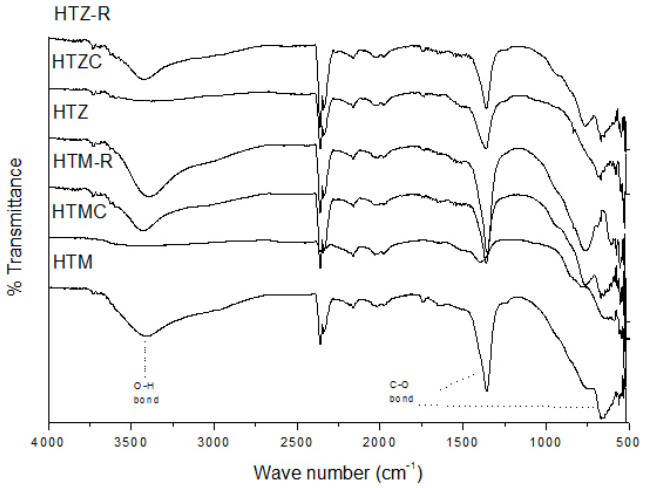

Fig. 3. FTIR spectra of HTM and HTZ, thermally treated and reconstructed samples.

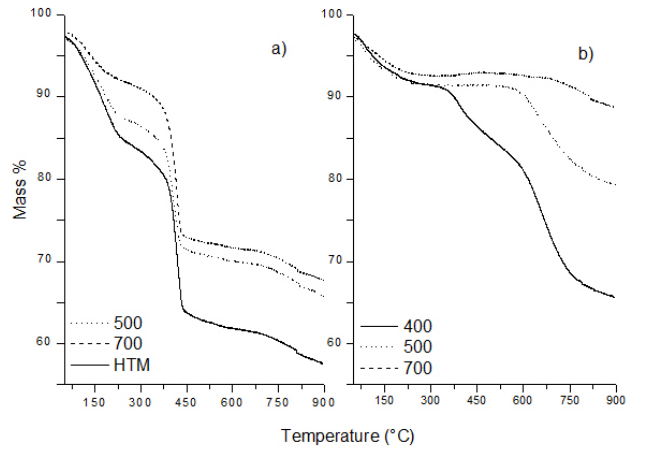

Fig. 4. TG analyses for thermally treated and reconstructed HTM samples.

It was also possible to obtain a hydrotalcite Zn-Al (HTZ) from lab acid wastewater. A layered structure is observed, and the memory effect is maintained (HTZ-R). However, thermal treatment has an influence on d_{003} spacing and decreases after the hydrotalcite reconstruction.

3.3. FTIR spectra

The FTIR spectra of the samples obtained from lab acid wastewater by the co-precipitation method are depicted in Fig. 3. The spectra of the HTM and HTZ samples that were thermally treated (HTMC and HTZC) and reconstructed using water (HTM-R and HTZ-R) were similar to those reported in the literature [14], and all of the spectra showed characteristic bands due to hydrotalcite-like compounds. The intensity of the broad band at *ca.* 3,400 cm^{-1} is due to the stretching mode of hydroxyl groups of the brucite layers; the very weak band at 1,600 cm^{-1} corresponds to the bending mode of water molecules from the interlayer. The weakness of this band should be related to the small amount of water remaining in the hydrophobic interlayer. Other bands are recorded at 1,250 cm^{-1} for C-(O)-O groups [14]. In addition, FTIR spectroscopy was able to provide information about the short-range order, which was dependent on the coupling of a vibration mode to adjacent vibrations. The use of lab acid wastewater has no influence on the structure of HT; the only influence was observed in thermally treated samples in which O-H vibrations were lost by dehydration route, but both materials were recovered in the reconstruction process [24], so this technique confirmed that the memory effect was present for the HTM and HTZ samples.

3.4. Thermal analyses

Thermal analyses of samples were measured in thermally treated products at 500°C and 700°C (Fig. 4(a)) because in this temperature range the decomposition process can be observed. Moreover, for higher temperatures, HTM samples can be degradated and not allowed to enter a reconstruction process. The decomposition of HTM could be attributed to the dehydroxylation and decarbonation of the material. In the dehydration process of HTM samples, its two characteristic steps could be observed: the first one, at 310°C (18%), was due to the bond between the hydrogen in water and the hydrotalcite hydroxyl surface; meanwhile, the second, at 450°C (36%), was probably due to a decarbonation process [25]. Both processes were identified in thermally treated samples. In the case of the 500°C thermally treated sample, the first loss was observed at 250°C (12%) and the second at around 445°C (28%). On the other hand, for the 700°C thermally treated sample, the first step appeared at 210°C (7%) and the second at 455°C (26%). The change in the weight loss for HTM at 500°C and 700°C due to the dehydroxilation process is associated with the water and hydrogen structurally bonded in the interlayer space, which is lost during the thermal process.

As for the rehydrated samples, TG analyses showed the same process for the weight loss (Fig. 4(b)). In the 400°C reconstructed sample, the first loss appeared at around 195°C (8%), the second loss at 470°C (16%), and the last one at 750°C (32%). In the 500°C reconstructed sample, the first weight loss appeared at 180°C (9%) and the second at 760°C (17%). Finally, in the 700°C sample, the first loss was found at 220°C (7%) and the last one at 820°C (9%). Similarly, for the reconstructed samples, the first loss was due to the dehydroxylation process and the second loss was due to the decarbonation process [25]. Nevertheless, in the 700°C reconstructed sample, the weight loss was less clear. From these results, it is evident that reconstructed hydrotalcites had better thermal stability. Nonetheless, the samples that were thermally treated at higher temperatures and reconstructed did not show a significant change, which is presented in Fig. 3. Finally, it is possible to confirm that hydrotalcites synthesized from the lab acid wastewater show a similar thermal behavior to hydrotalcites prepared using clear water.

3.5. Surface area and SEM

The BET surface area was found at 52.23 and 49.71 m^2/g, and mean diameter pore was 10.61 and 7.81 nm, for HTM and HTZ, respectively. From these results, it was evident that the HTM had the highest BET surface area and largest pore diameter, which will facilitate both diffusion and adsorption of phenol and chromium (VI) inside the HTM. After 48 h of contact with the adsorption test, BET surface area changed to 15.98 and 31.36 m^2/g, and mean diameter pore was 9.67 and 9.91 nm for HTM and HTZ, respectively. These results showed that the highest surface area and pore diameter were for the HTZ adsorbent. This was due to the adsorption process which led to the decrease of the surface area. Meanwhile, for HTM, whose removal process resulted in a larger quantity for both compounds, the pores may be covered by the adsorption of phenol and chromium (VI) molecules.

Scanning Electron Microscopy (SEM) pictures of HTMC and HTZC after 10 min and 48 h of contact time with phenol and chromium (VI) are shown in Fig. 5. The morphologies of both compounds are a random tiny filament arrangement in the HT, no pores are visible. The images showed that the composition in both HTs, MgAl (HTM) or ZnAl (HTZ), did not change their morphologies. As for HTM (Fig. 5(a)), the tiny filaments resulted less than 1 μm in length, whereas in HTZ (Figs. 5(b),(c)) they were found at around 1 μm. This is in agreement with BET surface area results – particles in HTM were smaller than in HTZ, so surface area was higher; also, in their micrographs were observed aggregates on the surface associated to the phenol and chromium (VI) ions, which were removed better with HTM.

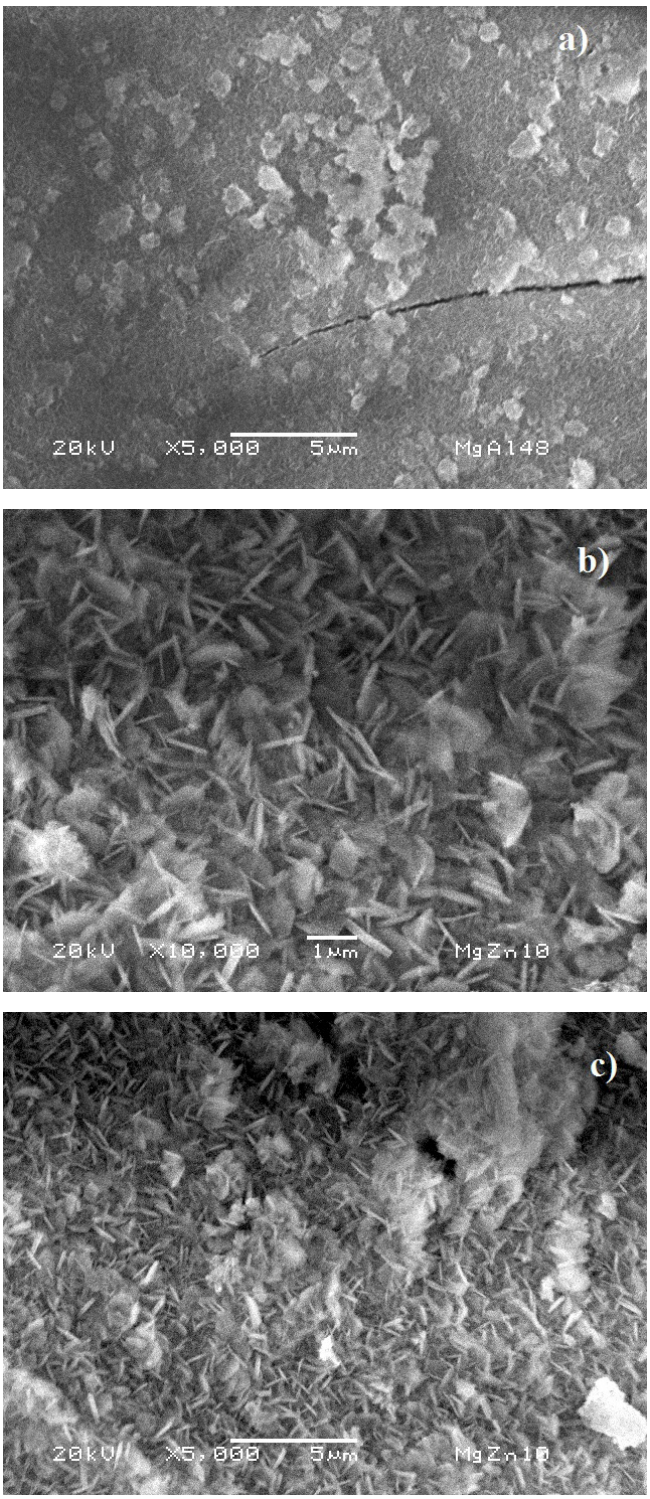

Fig. 5. SEM images for: (a) HTMC after 48 h of adsorption contact, and HTZC after 10 min contact at (b) 10,000x and (c) 5,000x.

3.6. Adsorption test

Table 3 shows the adsorption data of phenol and chromium (VI)compounds by HTMC and HTZC. There was an almost complete removal of both compounds by these two hydrotalcites at long periods of time (48 h). The high adsorption ability of thermally treated hydrotalcite was due to a lack of carbonate ion interaction, which was absent in the interlayer space. As mentioned before, the thermal process caused the collapse of layered structures, which resulted in amorphous phases of Mg-Al or Zn-Al oxides [17]. In addition, the amounts of phenol and chromium (VI) increased as a function of time [26]. The initial pH of the solution was 6 and was not adjusted for the adsorption test because the main topic of

Table 3
Adsorption data for phenol and chromium (VI) removal

Sample	Time (h)	Final pH	Phenol C_i = 50 mg/L		Chromium (VI) C_i = 10 mg/L	
			C_s (mg/g)	% adsorption	C_s (mg/g)	% adsorption
HTMC	0.5	10.7	46.2	92.4	3.1	31.0
	2.0	10.5	45.1	90.1	5.7	56.7
	48	10.7	46.7	93.4	9.4	93.8
HTZC	0.5	10.3	41.5	83	1.0	9.8
	2.0	10.6	45.3	90.7	5.4	53.5
	48	10.6	45.1	90	8.9	88.9

this paper is hydrotalcite synthesis from lab acid wastewater. However, the final pH increased by 10 units. This is typical behavior in adsorption processes and is due to a partial dissolution of Mg^{2+}, Al^{3+}, or Zn^{2+} ions (in solution), but a higher pH value enhanced competition of hydroxides with phenol and chromium for active sites on the adsorbent. Also, CO_3^{2-} and OH^- anions have an influence in adsorption processes because the memory effect caused these ions to resume their original structure due to the high affinity among them. This has a significant impact on the adsorption process, since real competition existed in the interlayer space between carbonates, hydroxyl, phenol and chromium (VI) ions.

The adsorption time of phenol in HTMC for a short period of time (0.5 h) reached 92% and was almost the same for a long period of time (48 h) at 93%. In the case of HTZC, the obtained results were similar, and adsorption changed from 83% to 90% for short and long periods of time, respectively. At the beginning, phenol and chromium (VI) molecules quickly occupied an adsorbant surface and the internal sites [27]; so, for short periods of time, adsorption process was fast; whereas for long periods of time, there were few sites and the adsorption reached an apparent equilibrium. Nonetheless, time had a real influence in chromium adsorption; therefore, HTMC only reached 31% for a short period of time and improved for long periods of time up to 93%, which was the same behavior found in the case of HTZC. This effect is due to the hydrotalcite-like compound's affinity to carbonate, phenol and chromium (VI), since hydrotalcites can remove these pollutants with their memory properties. Chromium (VI) ion had less attraction for HT and there were fewer chromium than phenol molecules because it took more time to adsorb them in a lamellar structure and it only got some active adsorption sites. In general, the adsorption capacity of HTZC was lower than that of HTMC because of the partial dissolution of the sheets, or ZnO crystallization during the reconstruction process increased in HTZC, as it is shown by X-ray diffraction results in Fig. 2.

The effect of the initial phenol or chromium (VI) concentration (50 or 10 mg/L) on the adsorption capacity is shown in Table 3. For LDH or HT materials, the amount of removal was linearly proportional to the initial concentration [27,28]. It can be seen that the adsorption capacity of phenol increased as a function of the chromium (VI) concentration, which was added in lower concentrations. The adsorption capacity was augmented as the initial concentration of the anion, phenol or chromium (VI) increased. All materials, as well as HT, had limited available adsorption sites, initial phenol concentration was 5 times greater than that of chromium (VI); thus, adsorption equilibrium was preferred for phenol, which occupied a large number of available sites, while Cr (VI) occupied only few sites. The results showed that the hydrotalcite-like compound synthesized from lab acid wastewater had phenol and chromium (VI) anions. The prepared adsorbents could be considered to control these anions, which were thought-of as pollutants in water generated in the same laboratory.

The adsorption data as phenol and Cr (VI) concentration in a separated solution were analyzed using the Freundlich and Langmuir adsorption isotherm models to obtain maximum adsorption capacity:

$$\frac{C_e}{C_s} = \frac{C_e}{C_m} + \frac{1}{C_m L} \tag{2}$$

where C_e is the concentration of phenol or Cr (VI) in solution (mg/L), C_s is the amount of phenol or Cr (VI) in the LDH (mg/g), L and C_m are Langmuir constants, which are related to adsorption energy.

$$\log C_s = \log K_f + n_f \log C_e \tag{3}$$

where C_s is the amount of phenol or Cr (VI) in the LDH, C_e is the concentration of phenol or Cr (VI) in solution (mg/L), n_f and K_f are Freundlich constants, which are related to adsorption intensity and the relation with adsorption capacity.

From the literature, it has been found that the best adsorption capacity was reported for thermally treated HT (10). In Table 4 only the adjustment for these samples is reported. The best adjustments for HTMC and HTZC were obtained by the Langmuir model, which explains that if $0<b<1$, the adsorption process is thermodynamically favorable. In our case, parameter b was in this range of phenol and chromium (VI). For chromium (VI) both models showed the adsorption maximum at 5.9 for HTMC and 2.09 for HTZC, which were far from those reported by Goh [29] [120 mg/g] and in a previous paper by Martínez-Gallegos [30] [78 mg/g], but this result confirms that the memory effect plays an important role in the adsorption process. Freundlich constant N_f was not higher than 1, so the adsorption process was not favorable. In the case of phenol, N_f constant was greater than that of chromium (VI), resulting in a preferred adsorption process onto HT. Also for phenol, the observed C_s is in accordance to the other similar experiments reported [60–200 mg/g] [1,31]. Nevertheless, HTMC showed better adsorption capacity

Table 4
Freundlich and Langmuir parameters for phenol and chromium (VI) adsorption

		Freundlich			Langmuir		
		K_f (mg/g)	N_f	R^2	Q_m (mg/g)	b	R^2
Phenol	HTMC	3.32	0.955	0.951	111	0.031	0.973
	HTZC	2.66	0.988	0.919	83.3	0.035	0.942
Cr (VI)	HTMC	0.60	0.755	0.976	5.92	0.082	0.983
	HTZC	0.45	0.495	0.931	2.09	0.186	0.933

Table 5
Phenol and chromium (VI) adsorbed by hydrotalcite-like compounds and bio-materials

Anion	Adsorbed quantity	Material	Author
Cr (VI)	4.95 mg/L	Water hyacinth	[3]
Phenol	9.9 mg/L		
Phenol	196 mg/L	Corn cob silica and alginate	[1]
Cr (VI)	0.78 mmol/g	Hydrotalcite MgAl calcined at 450°C	[23]
	0.097 mmol/g	Hydrotalcite ZnAl calcined at 450°C	
Cr (VI)	128 mg/g	Mg-Al-CO_3 hydrotalcite	[31]
Cr (VI)	6.5 mg/g	Mg-Al hydrotalcite	[32]
	6.8 mg/g	Mg-Al gibbsite hydrotalcite	
Bisphenol A	67 mg/g	Dodecylsulfate ion-intercalated hydrotalcite-like compound	[33]
Cr (VI)	5.9 mg/L	Calcined hydrotalcite HTMC	This work
Phenol	111 mg/L		

than HTZC, which was in agreement with X-Ray diffraction results, where HTZC showed a reduced interplanar distance that made it difficult for phenol and chromium species to be adsorbed.

For both materials, HTMC and HTZC, the adsorption capacities were found in the same range of other similar materials, as shown in Table 5. Only the bio-adsorbents that exceed hydrotalcite-like compounds may be greater due to the surface area, which was larger than that of some clay materials.

4. Conclusions

In this study, the synthesis of hydrotalcite-like compounds HTM and HTZ using acidic wastes from a lab has been realized, and the structure of the obtained materials was similar to that of hydrotalcite-like materials. For HTM, XRD analysis showed that the layered structure was lost during thermal treatment; the loss started at 400°C, but the structure was reconstructed after contact with water. This behavior corresponded to a memory effect, which plays an important role in phenol and chromium (VI) adsorption. Also, by the same technique, HTM or HTZ materials did not have any substantial changes or differences in their structure, and additional peaks were not observed. The vibrational bands for HT materials were identified for both HTM and HTZ. In TG analyses, the two characteristic weight losses, dehydration and decarbonation, were observed in these materials. On the other hand, the adsorption process demonstrated a real influence with the initial concentration of the removed anion, phenol, or chromium (VI). Hence, for a short period of time (0.5 h), phenol adsorption was the most important process in HTM. It was proved that 90% or more of the initial concentration (50 mg/L) was adsorbed at this time. Meanwhile, chromium (VI) only reached 31% adsorption at the same time. Surface area and SEM micrographs confirmed this behavior. HTM showed small particles and higher BET area than HTZ, whose characteristics helped to increase adsorption capacity. Finally, as the initial concentration was increased, adsorption capacity also increased.

The hydrotalcite-like compounds synthesized from lab acid wastewater by the co-precipitation method reached two initial proposals: lab acidic wastes were used in HT synthesis to reduce their quantities, and the obtained product was available for the adsorption process of metals or organic compounds. The HTM and HTZ showed the same properties as the other LDH materials.

References

[1] J. Shim, J.M. Lim, P.J. Shea, B.T. Oh, Simultaneous removal of phenol, Cu and Cd from water with corn cob silica-alginate beads, J. Hazard. Mater., 272 (2014) 129–135.
[2] A. Gupta, C. Balomajumder, Simultaneous removal of Cr(VI) and phenol from binary solution using Bacilius sp. Immobilized onto tea waste biomass, J. Water Proc. Eng., 6 (2015) 1–10.
[3] A. Gupta, C. Balomajumder, Removal Cr(VI) and phenol using water hyacinth from single and binary solution in the artificial photosynthesis chamber, J. Water Proc. Eng., 7 (2015) 74–82.
[4] S. Golbaz, A.J. Jafari, M. Rafiee, R.R. Kalantary, Separate and simultaneous removal of phenol, chromium, and cyanide from aqueous solution by coagulation/precipitation: mechanisms and theory, Chem. Eng. J., 253 (2014) 251–257.

[5] D. Wan, Y. Liu, S. Xiao, J. Chen, J. Zhang, Uptake fluoride from water by calcined Mg-Al-CO_3 hydrotalcite: Mg/Al ratio effect on its structure, electrical affinity and adsorptive property, Coll. Surf. A, 469 (2015) 307–314.
[6] H.A. Asmaly, B. Abussaud, A. Ihsanullah, T.A. Saleh, V.K. Gupta, M.A. Atieh, Ferric oxide nanoparticles decorated carbon nanotubes and carbon nanofibers: from synthesis to enhanced removal of phenol, J. Saudi Chem. Soc., 19 (2015) 511–520.
[7] J. Lee, K.A. Min, S. Hong, S. Kim, Ab initio study of adsorption properties of hazardous organic molecules on graphene: phenol, phenyl azide, and phenylnitrene, Chem. Phys. Lett., 618 (2015) 57–62.
[8] W. JianSong, X. YingKai, W. JianYu, W. LiRong, The growth mechanism of hydrotalcite crystal, Sci. China Technol. Sci., 55 (2012) 872–878.
[9] Y.X. Zhang, X.D. Hao, M. Kuang, H. Zhao, H. Wen, Preparation, characterization and dye adsorption of Au nanoparticles/ZnAl layered double oxides nanocomposites, Appl. Surf. Sci., 283 (2013) 505–512.
[10] Y. Yang, N. Gao, W. Chu, Y. Zhang, Y. Ma, Adsorption of perchlorate from aqueous solution by the calcinations product of Mg/(Al-Fe) hydrotalcite-like compounds, J. Hazard. Mater., 209–210 (2013) 318–325.
[11] T.S. Anirudhan, P.S. Suchithra, Synthesis and characterization of tannin-immobilized hydrotalcite as a potential adsorbent of heavy metal ions in affluent treatments, Appl. Clay Sci., 42 (2008) 214–223.
[12] R. Salomao, L.M. Milena, M.H. Wakamatsu, V.C. Pandofelli, Hydrotalcite synthesis via co-precipitation reactions using MgO and $Al(OH)_3$ precursors, Ceram. Int., 37 (2011) 3063–3070.
[13] S.P. Paredes, G. Fetter, P. Bosch, S. Bulbulian, Sol-gel synthesis of hydrotalcite-like compounds, J. Mater. Sci., 41 (2006) 3377–3382.
[14] M. Herrero, S. Martínez-Gallegos, F.M. Labajos, V. Rives, Layered double hydroxide/polyethylene terephthalate nanocomposites. Influence of the intercalated LDH anion and the type of polimerization heating method, J. Solid State Chem., 184 (2011) 2862–2869.
[15] Environment and Natural Resources Secretary, Mexican Official Law NOM-002-SEMARNAT-1996. Accessed on June 11, 2015, Available online at: http://www.conagua.gob.mx/CONAGUA07/Noticias/NormasOficialesMexicanas.pdf
[16] Health Secretary, Mexican Official Law NOM-127-SSA1-1994. Accessed on June 6, 2015, Available online at: http://www.salud.gob.mx/unidades/cdi/nom/127ssa14.html
[17] S. Martínez-Gallegos, H. Pfeiffer, E. Lima, M. Espinosa, P. Bosch, S. Bulbulian, Cr(VI) immobilization in mixed (Mg, Al) oxides, Microporous Mesoporous Mat., 94 (2006) 234–242.
[18] T. Stanimirova, G. Kirov, Cation composition during recrystallization of layered double hydroxides from mixed (Mg, Al) oxides, Appl. Clay Sci., 22 (2003) 295–301.
[19] F. Teodorescu, A.M. Paladuta, O.D. Pavel, Memory effect of hydrotalcites and its impact on cyanoethylation reaction, Mat. Res. Bull., 48 (2013) 2055–2059.
[20] F. Cavani, F. Trifiro, A. Vaccari, Hydrotalcite-type anionic clays: preparation, properties and applications, Catal. Today, 11 (1991) 173–301.
[21] Z.Q. Zhang, H.Y. Zeng, X.J. Liu, S. Xu, C.R. Chen, J.Z. Du, Modification of MgAl hydrotalcite by ammonium sulfate for enhancement of lead adsorption, J. Taiwan Int. Chem. Eng., 60 (2016) 361–368.
[22] S. Miyata, A. Okada, Synthesis of hydrotalcite-like compounds and their physic-chemical properties-the systems Mg^{2+}-Al^{3+}-SO_4^{2-} and M^{2+}-Al^{3+}-CrO_4^{2-}, Clay. Clay Miner., 25 (1977) 14–18.
[23] D. Carriazo, M. Del Arco, C. Martín, V. Rives, A comparative study between chloride and calcined carbonate hydrotalcites as adsorbents for Cr(VI), Appl. Clay Sci., 37 (2007) 231–239.
[24] Q. Guo, Q. Guo, Water defluoration by hydrotalcite and takovite and subsequent formation of new fluoride-bearing phases, Environ. Technol., 34 (2014) 1053–1062.
[25] S.J. Palmer, L.M. Grand, R.L. Frost, Thermal analysis of hydrotalcite synthesized from aluminate solutions, J. Therm. Anal. Calorim., 103 (2011) 473–478.
[26] L. Xiao, W. Ma, M. Han, Z. Cheng, The influence of ferric iron in calcined nano-Mg/Al hydrotalcite on adsorption of Cr (VI) from aqueous solution, J. Hazard. Mater., 186 (2011) 690–698.
[27] Gh. Eshaq, A.M. Rabie, A.A. Bakr, A.H. Mady, A.E. ElMetwally, Cr(VI) adsorption from aqueous solutions onto Mg-Zn-Al LDH and its corresponding oxide, Desal. Wat. Treat., 57 (2015) 1–11. doi: 10.1080/19443994.2015.1110840
[28] A.A. Bakr, Gh. Eshaq, A.A. Mady, A.E. ElMetwally, Copper ions removal from aqueous solutions by novel Ca-Al-Zn layered double hydroxides, Desal. Wat. Treat., 57 (2015) 1–12. doi: 10.1080/19443994.2015.1051126
[29] K.H. Goh, T.T. Lim, Z. Dong, Application of layered double hydroxides for removal of oxyanions, Water Res., 42 (2008) 1342–1368.
[30] S. Martínez Gallegos, S. Bulbulian, Chromium (VI) separation from tannery wastes utilizing hydrotalcites, Sep. Sci. Technol., 52 (2004) 667–681.
[31] E. Álvarez-Ayuso, H.W. Nugteren, Purification of chromium (VI) finishing wastewaters using calcined and uncalcined Mg-Al-CO_3-hydrotalcite, Water Res., 39 (2005) 2535–2542.
[32] I. García-Sosa, M.T. Olguin, Comparison between the Cr(VI) adsorption by hydrotalcite and hydrotalcite-gibsite compounds, Sep. Sci. Technol., 50 (2015) 2631–2638. doi: 10.1080/01496395.2015.1066810
[33] Y. Li, H. Yu Bi, S. Long Shen, Removal of bisphenol A from aqueous solution by dodecylsufate ion-intercalates hydrotalcite-like compound, Environ. Technol., 33 (2012) 1367–1373.